Soot Volume Fractions in the Overfire Region of Turbulent Diffusion Flames

Y. R. SIVATHANU and G. M. FAETH

Department of Aerospace Engineering, The University of Michigan, Ann Arbor, MI 48109-2140

Overfire soot volume fractions and mixture fractions, flame heights, and characteristic flame residence times, were measured for turbulent acetylene, propylene, ethylene and propane diffusion flames burning in still air. Test conditions ranged from highly buoyant pool-like flames to buoyant jet flames, using three burners (with exit diameters of 5, 50, and 234 mm) and a wide range of fuel flow rates. Soot generation efficiencies (the percentage of fuel carbon converted to soot and emitted from the flame) were uniform throughout the overfire region for a given flame condition. Soot generation efficiencies increased with increasing flame residence times but tended to approach asymptotic values for residence times roughly ten times longer than residence times at the normal smoke point. Within the asymptotic region, soot volume fractions are directly related to mixing levels, analogous to the laminar flamelet concept for nonpremixed flames, which offers substantial simplifications for analysis of the continuum radiation properties of the overfire region.

NOMENCLATURE

a acceleration of gravity
C_p specific heat at constant pressure
d burner exit diameter
d_p soot particle diameter
f mixture fraction
f_v soot volume fraction
L flame height
M_i moles of species i for stoichiometric combustion
$\dot{Q}_f$ heat release rate
Q^* dimensionless heat release parameter (Eq. 1)
Q_r radiative heat loss fraction
r radial distance
Re burner Reynolds number
Ri burner Richardson number
T temperature
u streamwise velocity
x height above burner

Greek Symbols

λ wavelength
ν kinematic viscosity
ρ density
τ_r characteristic flame residence time

Subscripts

c centerline value
f fuel
o burner exit condition, oxygen
∞ ambient condition

Superscripts

$(\bar{})$ time-averaged quantity
$(\sim)$ Favre-averaged quantity

INTRODUCTION

Practical buoyant turbulent diffusion flames are generally luminous and emit significant continuum radiation from soot. In addition to soot temperatures and the complications of a turbulent environment, exact predictions of continuum radiation from soot would involve a variety of soot properties, e.g., concentrations, particle size and shape distributions, and refractive indices. Tien and Lee

Published by Elsevier Science Publishing Co., Inc.
655 Avenue of the Americas, New York, NY 10010

0010-2180/90/$3.50

[1], however, point out a useful approximation that makes the definition of soot properties more tractable, namely that continuum radiation from soot particles in flames is generally most significant in the infrared (wavelengths longer than 1000 nm) whereas soot particles are generally smaller than 100 nm so that the Rayleigh limit of small particles is a reasonable approximation for estimating the spectral absorption coefficients of soot and scattering can be ignored. Later work has provided some support for this approximation: an inverse dependence of light attenuation on wavelength, characteristic of the Rayleigh limit, has been observed for laminar ethylene–air and turbulent acetylene–air diffusion flames [2, 3]; and reasonable estimates of spectral emission in the continuum, based on the Rayleigh limit, have been obtained for turbulent ethylene–air and acetylene–air diffusion flames [3, 4]. Under this approximation, the only soot properties needed for radiation analysis are the real and imaginary parts of the refractive index of soot and soot volume fractions. There is controversy concerning the refractive indices of soot within flames [1, 5–9]; nevertheless, Tien and Lee [1] and Dalzell and Sarofim [5] find that they are relatively independent of the fuel for diffusion flames and provide values in good agreement with each other in the infrared where radiation effects are most significant. Thus, the present investigation considered soot volume fractions because less information is available concerning this property. The study was limited to soot volume fractions within the overfire region of buoyant turbulent diffusion flames burning in still air.

Detailed analysis to find soot volume fractions in turbulent flames would involve treating complex heterogeneous chemistry in a turbulent environment. Use of the conserved-scalar formalism of nonpremixed flames, in conjunction with the laminar flamelet concept, however, has the potential for making this seemingly interactable problem accessible—at least for the purposes of flame radiation predictions. The key hypothesis of the laminar flamelet concept is that instantaneous scalar properties are only functions of mixture fraction—called state relationships [10–13]. It has been observed that except near points of flame attachment or quenching, the concentrations of major gas species can be correlated to yield nearly universal state relationships for a variety of fuels burning in air [10–17]—even for heavily sooting fuels like acetylene and ethylene [3, 4, 18]. Near-equilibrium concentrations of major gas species are observed for nonhydrocarbon fuels and for fuel-lean conditions with hydrocarbon fuels, providing some rationale for the existence of state relationships for these conditions. However, equilibrium is not maintained for fuel-rich conditions with hydrocarbon fuels due to relatively slow processes of fuel decomposition and soot chemistry when mixture temperatures are low. Nevertheless, departures from chemical equilibrium of the concentrations of major gas species are still nearly universal yielding acceptable state relationships for a wide range of flame conditions.

The existence of state relationships for major gas species, in the presence of effects of fuel decomposition and finite-rate chemistry in fuel-rich regions, prompted earlier studies in this laboratory concerning the existence of more-or-less universal state relationships for soot volume fractions [3, 4, 18]. Measurements in laminar jet flames of acetylene and ethylene showed that soot volume fractions were only appreciable for a relatively narrow range of mixture fractions in the fuel-rich region (soot spikes) near the stoichiometric condition [3, 4]. State relationships were found within the soot spikes although the correlations were poorer than for major gas species. This was attributed to effects of finite-rate chemistry, laminar hydrodynamics associated with the small diffusivity of soot particles, and effects of thermophoresis of soot particles. Subsequently, soot volume fraction state relationships were studied for lean conditions in the overfire region of turbulent flames, based on measurements of mean mixture fractions and soot volume fractions [18]. Unfortunately, this study was hampered by several experimental difficulties. Near stoichiometric conditions, where instrument sensitivities were adequate, relationships between mean scalar properties are biased from the relationships between instantaneous scalar properties that are relevant to state relationships, due to effects of turbulent fluctuations. On the other hand, for lean conditions where effects of turbulent fluctuations are small, poorer instrument sensitivities

yielded large experimental uncertainties. Within these limitations, the findings tended to support the existence of universal soot volume fraction state relationships for lean conditions when residence times in the flame were sufficiently long (although necessary residence times were not quantified). Furthermore, estimates of flame radiation properties and soot concentrations in turbulent ethylene and acetylene flames, based on the approximate soot volume fraction state relationships, were also reasonably good [3, 4, 18], as noted earlier. Thus, some dispersion of soot volume fraction state relationships apparently can be tolerated during computations of the radiation properties of turbulent flames.

The present investigation is an extension of Ref. 18 and considers the soot volume fraction state relationship concept in the overfire region of turbulent diffusion flames. The objectives were to examine the concept in the far-overfire region, where effects of turbulent fluctuations are small, for a broader range of fuel and flame conditions and with improved experimental accuracy in comparison to Ref. 18. The new measurements involved acetylene, propylene, ethylene, and propane flames burning in still air. Flames were observed using three different burners, having exit diameters of 5, 50, and 234 mm, with operating conditions ranging from buoyant jet flames to highly buoyant pool-like flames. This provided a wide range of flame residence times so that effects of finite-rate chemistry on soot properties in the overfire region could be studied. Flame heights and characteristic residence times were also measured, in order to define flame conditions and to assist interpretation of the other measurements.

The article begins with a description of experimental methods. Results are then considered, treating flame lengths and characteristic residence times first and then concluding with soot properties and examination of soot volume fraction state relationships.

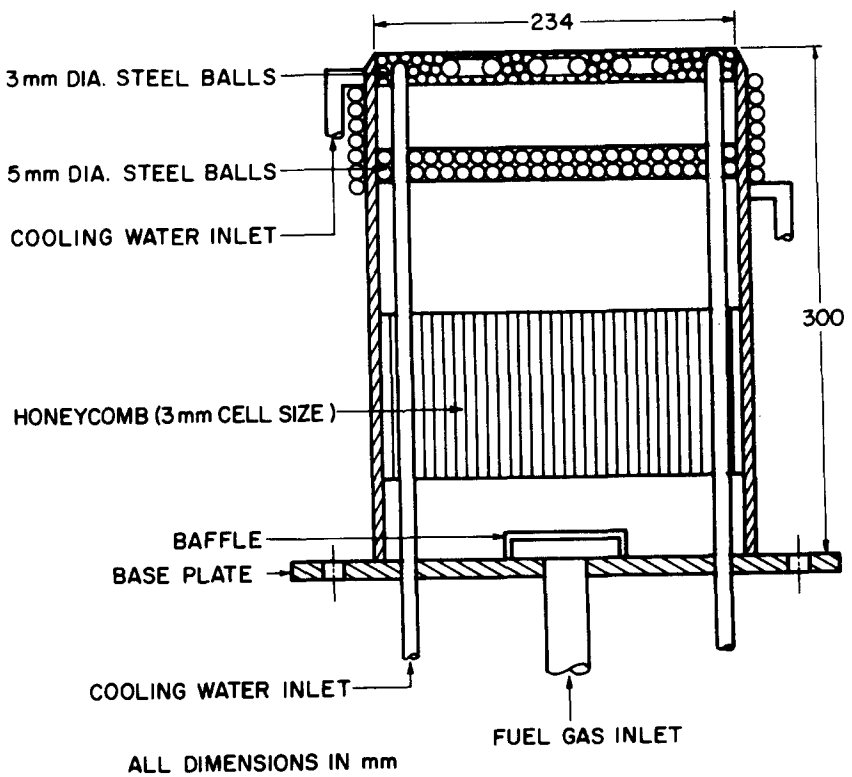

Fig. 1. Sketch of 234-mm-diameter burner.

EXPERIMENTAL METHODS

Apparatus

The test arrangement involved vertically upward injection of fuel in still air with the flames attached at the burner exit. The flames burned within a large enclosure (2.4×2.4×3.6 m high) with a metal hood and an adjustable exhaust system at the top to remove combustion products. Room disturbances of the flames were reduced using strips of plastic film, which terminated slightly above the floor, as the side walls of the enclosure, as well as a second enclosure (1×1×2 m high, one layer of screen, 630 wires per meter, 0.25 mm wire diameter) directly around the flames. Instrumentation was mounted rigidly; therefore, the burner was traversed horizontally and vertically (with positioning accuracies of 0.1 and 1 mm, respectively) to measure properties in the far-overfire region.

Three water cooled burners, having exit diameters of 5, 50, and 234 mm, were used to provide a variety of flame geometries and residence times. A sketch of the 234-mm-diameter burner appears in Fig. 1. The fuel entered a baffled plenum chamber at the bottom of the burner and passed through a honeycomb section (3 mm cell size, 100 mm long) to remove any residual swirl. The flow then passed through two more plenum sections and two beds of steel balls (5 and 3 mm diameter balls with bed heights of 40 mm) to provide a uniform flow at the burner exit. The burner was cooled by water flowing through a coil soldered to its outside surface as well as a second coil buried in the top bed of steel balls. The flames attached naturally on this burner. The 50-mm burner was similar to the arrangement shown in Fig. 1: the flames attached naturally at the exit of this burner as well. The 5-mm-diameter burner was used during the earlier study of the overfire region of sooting flames [18] and is described in detail by Jeng [19]: a small coflow of hydrogen was used to attach the flames at the exit of this burner, similar to Becker and Liang [20].

Properties of the fuels at the normal smoke point were also measured, using an open coflow burner developed by Gore [21]. The fuel flowed from a center tube, having an inside diameter of 14.3 mm and a wall thickness of 0.9 mm, while air flowed from a concentric port, having an inside diameter of 102 mm. Both flows passed through a 50-mm-deep bed of 2-mm-diameter stainless-steel balls, a 10-mm gap, and a 25-mm-long honeycomb (1 mm hexagonal cells, flush with the downstream end of the tubes).

Instrumentation

Measurements consisted of flame heights and residence times, using dark-field motion picture photography, mean soot volume fractions and mixture fractions in the overfire region, using an optical/sampling probe, and radiative heat fluxes and heat-loss fractions, using a radiation heat flux transducer.

Flame Photography

The test flames were luminous and were readily photographed in a darkened room to determine flame heights and flame residence times. Motion-picture photographs (100–500 pps with Kodak 4X film) were used with 100- or 1000-Hz timing marks on the film, depending on conditions.

Flame height measurements were obtained by averaging luminous flame heights observed on 100 pictures, obtained over a 5–10-s period. The experimental uncertainties (95% confidence) of the flame height determinations are estimated to be less than 10%.

Several measures of residence time in the flames were considered, along the lines of Becker and Liang [20], before deciding to base the characteristic flame residence time (called "residence time" in the following) on direct measurements. The present residence time was defined as the time interval between the interruption of the fuel flow and the disappearance of all flame luminousity. The flow of fuel was terminated by rapidly moving a shutter (located a few millimeters above the burner exit) across the exit of the flame. Shutter speeds allowed the leading edge of the shutter to cross the burner exit in less than 10 ms for the 5- and 10-mm-diameter burners and in less than 40 ms for the 234-mm-diameter burner. Camera speeds yielded less than 10 and 2 ms discretization errors on the films for turbulent and lami-

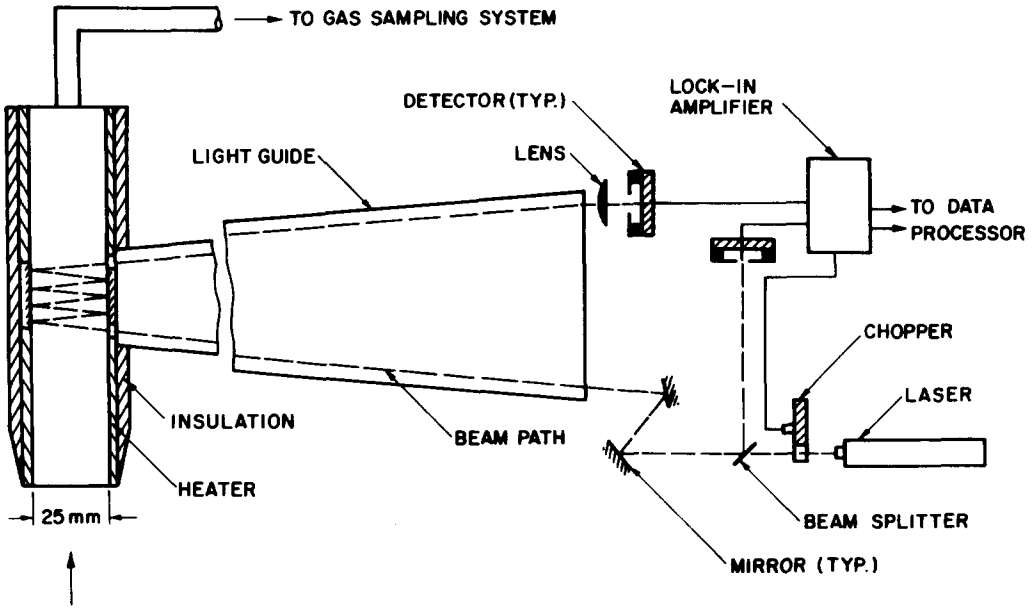

Fig. 2. Sketch of optical/sampling probe.

nar flames, respectively. Six tests were averaged to find the characteristic flame residence time for each flame condition. Experimental uncertainties (95% confidence) of the residence time measurements were dominated by the limited number of samples and are estimated to be less than 10%.

Optical/Sampling Probe

The optical/sampling probe was used for measurements of mean soot volume fractions and mixture fractions in the far-overfire region (for mean fuel-equivalence ratios less than 0.1 and mean temperatures less than 500 K), where relationships between mean and instantaneous scalar properties are the same. A sketch of the optical/sampling probe appears in Fig. 2. The system functions by continuously drawing a sample into a 25×25 mm passage where mean soot volume fractions are measured by laser extinction, and mean compositions and mixture fractions are measured by gas chromatography.

Soot volume fractions were measured by laser extinction using the 632.8 line of a HeNe laser (5 mW, Spectra Physics Model 120). The laser beam made several passes across the sample to achieve extinction levels that minimized experimental uncertainties (extinction levels near e^{-1}), with the number of passes adjusted by tilting the mirrors with set screws. The mirror surfaces were heated to prevent deposition of soot particles on them by thermophoresis. A two-detector system (Newport Model 982 Laser Power Meters) measured the laser beam intensity before and after passing through the sample to compensate for laser power variations. The detector for transmitted radiation had a large active area (100 mm^2) with response within 99% at ± 3 mm from the axis for an angular misalignment of $\pm 2°$, therefore, effects of beam steering by refractive index variations in the sample (which were small in any event) were negligible. Laser line filters, a chopper (Stanford Research Systems, Model SR540) operating at 1500 Hz, and a carrier amplifier system (Stanford Research Systems, Model SR510) were used to reduce effects of background radiation and to improve signal-to-noise ratios. Output signals were stored using a microcomputer, as follows: 500 samples (each) in clean air before and after accumulating 5000 samples over a 10-s period when the flame was present. This cycle was repeated ten times and averaged to obtain the final extinction coefficient for the test condition. The clear air measurements provided a check of the optical

quality of the laser path in the event that soot had contaminated the mirrors or windows.

Past multiline laser extinction measurements for the underfire region of acetylene and ethylene flames suggest that the optical size parameters of soot particles, $\pi d_p/\lambda$, are less than 0.5 at a wavelength of 632.8 nm [2, 3], so that discrepancies between Rayleigh and Mie scattering predictions of soot volume fractions are less than 15% [22]. Oxidation of soot as it passes through the flame zone into the overfire region causes a further reduction of soot particle sizes [23]; therefore, it appears to be justified to find soot volume fractions assuming the small-particle Rayleigh scattering limit [1]. The selection of soot refractive indices needed to compute soot volume fractions involves uncertainties, as noted earlier. Tien and Lee [1] and Dalzell and Sarofim [5] find that soot refractive indices for hydrocarbon diffusion flames are relatively independent of fuel type and temperature for H/C ranges spanning the present fuels. On the other hand, a recent refractive index measurement by Batten [6] for a kerosene diffusion flame is not in good agreement with the results of Refs. 1 and 5, with effects of H/C ratio cited as a potential source of the discrepancy. Furthermore, several recent measurements of refractive indices in premixed hydrocarbon flames indicate effects of fuel type, fuel-equivalence ratio, and residence time in the postflame region [7–9]. Because the environment of soot in premixed and diffusion flames is substantially different, however, the diffusion-flame results of Refs. 1 and 5 were felt to be most appropriate for present test conditions. Thus, effects of fuel type, temperature, and residence time were ignored, and in order to be consistent with earlier work in this laboratory [3, 4, 18] and other recent measurements of soot volume fractions in diffusion flames [2, 22–25], soot volume fractions were computed using the refractive index measurements of Dalzell and Sarofim [5], i.e., $1.547 - 0.56i$ at 632.8 nm. Uncertainties in soot volume fraction measurements were largely due to finite sampling times, the Rayleigh scattering approximations, and estimates of the refractive indices of soot: they are estimated (95% confidence) to be less than 30% (within differences of refractive indices observed in Refs. 1 and 5) and were repeatable within 20%.

Sampling for gas composition and mixture fraction measurements was not isokinetic, since local gas velocities were unknown, however, effects of doubling and halving sampling rates were negligible. Gas samples were filtered (to remove soot) and cooled (to remove water vapor) so that analysis was on a dry basis. The arrangement and operating conditions of the gas chromatograph, as well as methods of data reduction, were the same as in Gore [21]. Experimental uncertainties (95% confidence) are estimated to be less than 10% for gas concentrations and less than 20% for mixture fractions and were repeatable within these limits.

Radiative Heat Fluxes

A water-cooled, nitrogen-purged, radiative heat flux transducer (Medtherm, Model 64P-10-22) was used to measure total radiative heat fluxes. The probe had a sapphire window and a viewing angle of 150°. The probe was traversed around the flames, summing individual radiative heat flux measurements to find the radiative heat loss fractions of the flames, similar to past work [3, 4].

Test Conditions

Test conditions are summarized in Table 1. Flames for the 5-mm-diameter burner were turbulent everywhere and can be classed as buoyant jet flames but with significant effects of buoyancy since the surroundings were still. Flames for the 50- and 234-mm-diameter burners had low initial Reynolds numbers and exhibited large-scale pulsations typical of highly buoyant flows; however, the overfire region was turbulent. These characteristics are in accord with the Richardson number ranges of the burners, with the values for the 5-mm-diameter burner being less than unity while values for the two larger burners were greater than unity. Typical of buoyant flames [26], radiative heat loss fractions were nearly constant for a particular fuel. Flame residence times varied by roughly an order of magnitude: shorter residence times presented problems of flame attachment and limited spatial resolution of the optical/sampling probe, longer residence times involved unman-

TABLE 1

Test Conditions for Sooting Turbulent Diffusion Flames [a]

Burner Diameter (mm)	Reynolds Number[b]	Richardson Number[c]	Heat Release Rate (kW)	Radiative Heat Loss Fraction (%)	Residence Time (ms)[d]	Range of x/d
Acetylene						
5	4940–9200	$1.5\text{-}5.5 \times 10^{-4}$	10.1–18.9	56–59	57–72	242–395
50	105–840	22–1330	2.3–18.0	56–61	132–295	28.5–37.5
Propylene						
5	7830–22800	$1.0\text{–}8.6 \times 10^{-4}$	11.5–33.5	40–44	91–109	300–395
50	190–2170	13–1660	2.9–33.5	40–46	200–600	24.5–37.5
234	280–450	$3.1\text{–}7.9 \times 10^{4}$	21.1–33.5	40–43	277–422	6.65–7.70
Ethylene						
5	5060–15900	$0.6\text{–}6.2 \times 10^{-4}$	7.8–24.5	33–36	89–107	242–342
50	120–1520	7.8–1210	2.0–24.5	36–40	210–338	24.5–37.5
234	190–3101	$1.9\text{–}5.5 \times 10^{4}$	14.4–24.5	—	206–234	6.65–7.70
Propane						
50	200–1950	18–1700	3.4–32.7	25–28	214–660	24.5–37.5
234	400	44330	32.7	28	362	6.65–7.70

[a] Vertical fuel injection in still air at NTP. Acetylene: Commercial Grade, Detroit Welding Supply Co.; propylene and ethylene: Chemically Pure Grade, Linde Division of Union Carbide, and Air Products and Chemicals Co.; propane: Chemically Pure Grade, Matheson Gas Products. Measurements along axis and at $r/x = 0.08$.

[b] $\mathrm{Re} = u_0 d/\nu_0$ based on average velocity at burner exit and burner gas properties.

[c] $\mathrm{Ri} = ad/u_0^2$ based on average velocity at burner exit.

[d] Time between termination of fuel flow and disappearance of all flame luminosity.

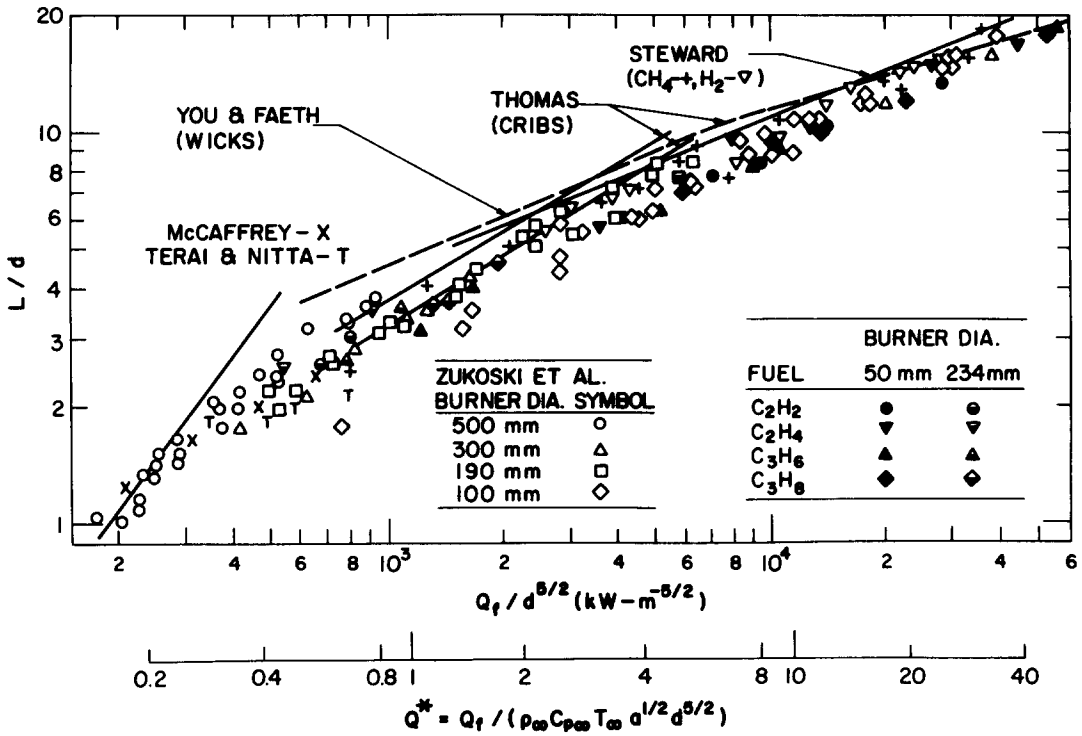

Fig. 3. Flame heights as a function of heat release rate for buoyant turbulent diffusion flames. Other data from Zukoski et al. [27], McCaffrey [28], Steward [29], Terai and Nitta [30], Thomas [31], and You and Faeth [32].

ageably large flames for present laboratory conditions. The optical/sampling probe measurements were made at $r/x = 0$ and 0.08 and x/d in the range 6.65–395, to examine whether relationships between soot volume fractions and mixture fractions varied within the far-overfire region.

RESULTS AND DISCUSSION

Flame Heights

Results concerning flame heights and residence times are considered first in order to help characterize the test conditions. However, this discussion is limited to the highly buoyant flames from the 50- and 234-mm-diameter burners because they are more typical of natural fires and satisfy relatively simple scaling relationships for buoyant flames. The buoyant jet flames from the 5-mm-diameter burner (having Richardson numbers less than unity) are less typical of natural fires and do not satisfy the scaling relationships of buoyant flames; nevertheless, this burner was useful for reaching short residence times during soot property measurements and findings from the small burner will be considered subsequently.

Flame heights for the 50- and 234-mm-diameter burners are illustrated in Fig. 3. The results are plotted according to the scaling relationships proposed by Zukoski et al. [27] for buoyant flames, e.g., L/d as a function of normalized heat release rate either in dimensional form, $\dot{Q}_f/d^{5/2}$, or using the following dimensionless heat release rate parameter:

$$Q^* = \dot{Q}_f/(\rho_\infty C_{p\infty} T_\infty (ad^5)^{1/2}). \quad (1)$$

Because ρ_∞, $C_{p\infty}$, T_∞, and a are constant for flames in still air, the dimensional and dimensionless heat release rate parameters are simply pro-

portional to one another. Earlier measurements for a variety of gaseous, liquid, and solid fuels are also shown on the plot, including those of Zukoski et al. [27], McCaffrey [28], Steward [29], Terai and Nitta [30], Thomas [31], and You and Faeth [32].

In view of the somewhat imprecise definition of visible flame height, and the resulting variation in the determination of this quantity by different techniques, or even by different individuals using the same technique, the correlation of the flame height measurements in Fig. 3 is quite good. Zukoski et al. [27] propose the following correlation based on their own measurements:

$$L/d = 3.3Q^{*2/3}, Q^* < 1;$$
$$L/d = 3.3Q^{*2/5}, Q^* \geq 1. \quad (2)$$

Present measurements are largely in the range $Q^* > 1$ and are in good agreement with Eq. 2 as well as the measurements of Zukoski et al. [27]. In this region, flame height is independent of d and largely depends on heat release rate, e.g., $L \propto \dot{Q}_f^{2/5}$, which is a well-known scaling relationship for buoyant flames [28]. Nevertheless, the geometry of the flames changes significantly as Q^* varies—approaching the appearance of buoyant jet flames at the largest values of Q^* illustrated in Fig. 3. Buoyant jet flames, however, are generally much longer, ca. $L/d \sim 100$ for hydrocarbons at the highest burner Reynolds numbers where flames can be attached at the burner exit, and their lengths are relatively independent of burner flow rate [20].

Residence Times

A correlation of flame residence times for the 50- and 234-mm-diameter burners was developed along the lines of Eq. 2 for flame heights. The residence time was assumed to be proportional to the ratio of a characteristic length scale, taken to be L, and a characteristic velocity. The properties of highly buoyant turbulent diffusion flames are not strongly influenced by burner exit velocities and molecular transport properties, while the driving potential for buoyancy forces, $\Delta\rho/\rho_\infty$, is essentially unity because densities within the flame are small in comparison to ambient densities. This implies that the characteristic velocity is a function of L, a, and the ratio of the volume flow rates of air and fuel for stoichiometric combustion—the last taken to be proportional to the ratio of the number of moles of oxygen and fuel for stoichiometric combustion, M_o/M_f. Replacing L by the burner diameter, using Eq. 2, then implies that the dimensionless residence time

$$\tau^* = \tau_r M_f (a/d)^{1/2}/M_0 \quad (3)$$

should be correlated as a function of Q^*.

Values of τ^* for the 50- and 234-mm-diameter burners are plotted as a function of Q^* in Fig. 4. The correlation is seen to be reasonably good and can be summarized by the following expression:

$$\tau^* = 560Q^{*1/3}; \quad 0.4 < Q^* < 60. \quad (4)$$

Based on Eq. 2, the correlation of Eq. 4 is appropriate for the range $1.8 \leq L/d \leq 17$.

Similar to the results for flame heights, the residence times for the buoyant jet flames on the 5-mm-diameter burner could not be correlated in the same manner as the buoyant flames produced by the larger burners. The residence times for the buoyant jet flames tend to increase with burner flow rate at first but reach a maximum and subsequently decrease with increasing flow rates since flame heights eventually become constant for momentum-dominated turbulent jet flames.

Soot Properties

The present optical/sampling probe measurements were limited to the far overfire region where no flame luminousity was ever seen, where differences between time averages and mass-weighted (Favre) averages are small, and where relationships between time-averaged scalar properties and instantaneous scalar properties are the same. Time-averaged gas temperatures at the sampling points were generally less than 500 K, which is also well below the 1300 K limit where soot oxidation is thought to be quenched [33]; therefore, soot behaves like a passive scalar in the overfire region, with variations of soot volume fractions only

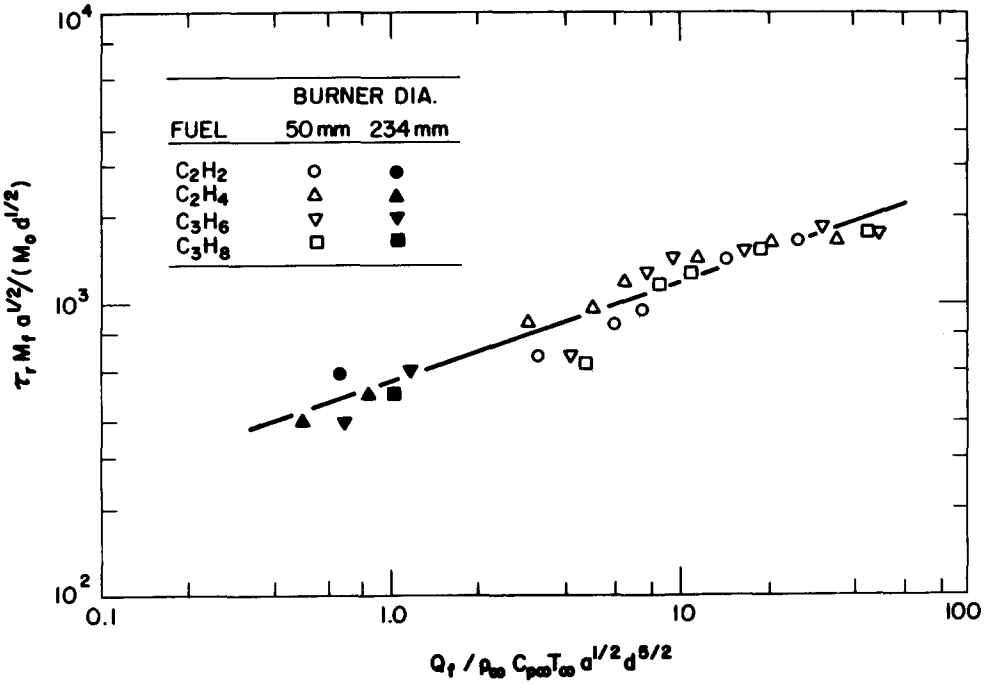

Fig. 4. Characteristic flame residence times as a function of heat release rate for buoyant turbulent diffusion flames. Line is correlation of Eq. 4.

caused by variations of soot concentrations at the point where soot oxidation reactions are quenched, and the extent of mixing with the surrounding air.

Present measurements of the correlation between soot volume fractions and mixture fractions (the soot volume fraction state relationship coordinates) in the far overfire region are illustrated in Figs. 5–8. It was found that the hydrogen coflow used to attach the flames for the 5-mm-diameter burner tended to reduce soot concentrations similar to earlier work with this burner [3, 4]. The results illustrated in Figs. 5–8 are corrected for this effect by making measurements for a range of hydrogen flow rates with this burner and then extrapolating the results to no hydrogen flow. This extrapolation was reasonable because soot concentrations varied nearly linearly with hydrogen flow rate for the low flow rates used to attach the present flames. The data were obtained at various x/d and r/x as noted in Table 1; however, data points are only identified by burner diameter and Reynolds number in order to reduce cluttering of the figures. Present measurements for acetylene with the 5-mm-diameter burner have been supplemented by earlier results using laser extinction tomography [18]: the earlier and present measurements are in good agreement in the region where they overlap.

Several soot volume fraction state relationship correlations are illustrated along with the measurements in Figs. 5–8. This includes the correlations proposed by Gore and Faeth [3, 4] for acetylene (Fig. 5) and ethylene (Fig. 7), where the prominent soot spikes for fuel-rich conditions were found by correlating measurements in laminar flames. Unfortunately, similar data for fuel-rich conditions are not available for propylene and propane. The correlations for lean conditions are based on the following assumptions: constant soot generation efficiency (defined as the mass fraction of fuel carbon that is emitted as soot from the flame), constant soot density (taken to be 1100 kg/m^3 from Newman and Steciak [34]), and no reaction or change of optical properties of soot in the lean (overfire) region. The correlations for lean conditions are based either on negligible heat losses from the flame or on radiative heat loss fractions at each point in the flame being equal to the

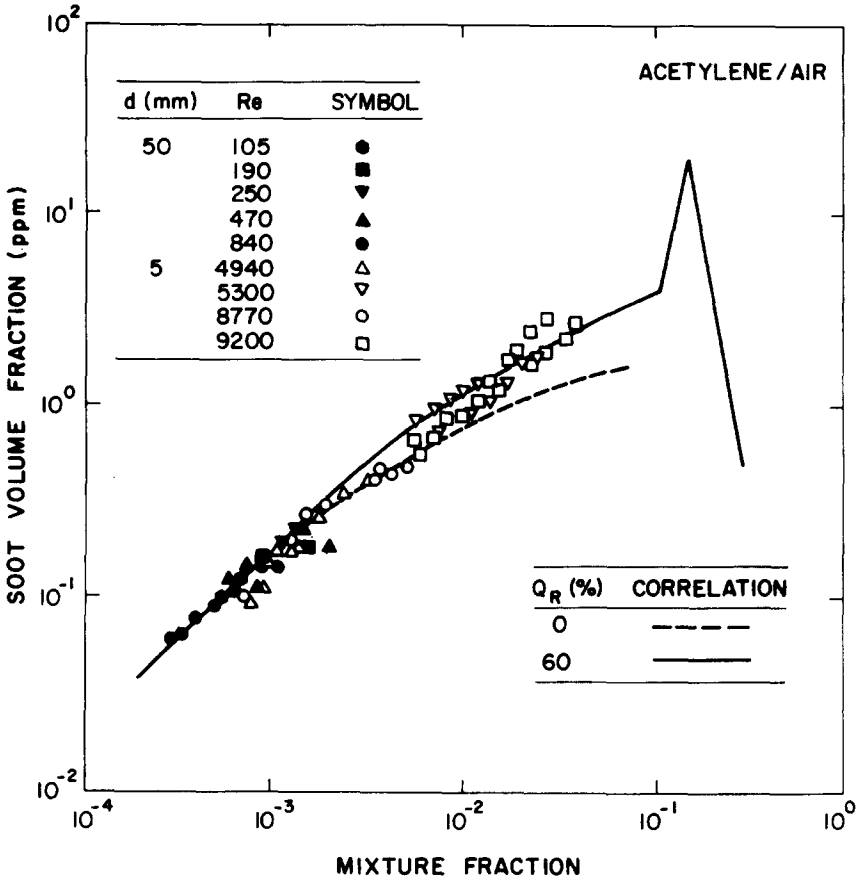

Fig. 5. Soot volume fraction state relationships for turbulent acetylene-air diffusion flames.

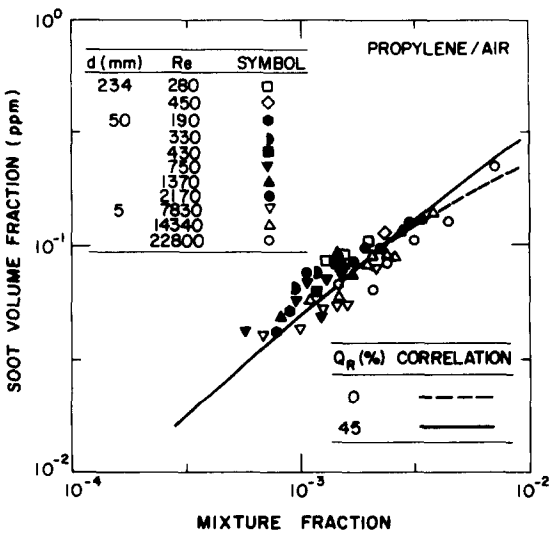

Fig. 6. Soot volume fraction state relationships for turbulent propylene-air diffusion flames.

value measured for the flame as a whole. The differences between the two correlations, however, are small in the region where present measurements were made.

The acetylene measurements (Fig. 5) were limited to the 5- and 50-mm-diameter burners due to problems of operating the 234-mm burner with this heavily sooting fuel. The results yield an excellent correlation between soot volume fractions and mixture fractions in the overfire region for a variety of flame conditions, implying that the laminar flamelet concept for soot volume fractions may be viable in the overfire region for this strongly sooting material. Furthermore, because soot is a passive scalar in the overfire region, the universal behavior seen in Fig. 5 means that soot volume fractions and mixture fractions have constant values when soot oxidation quenches, for various lo-

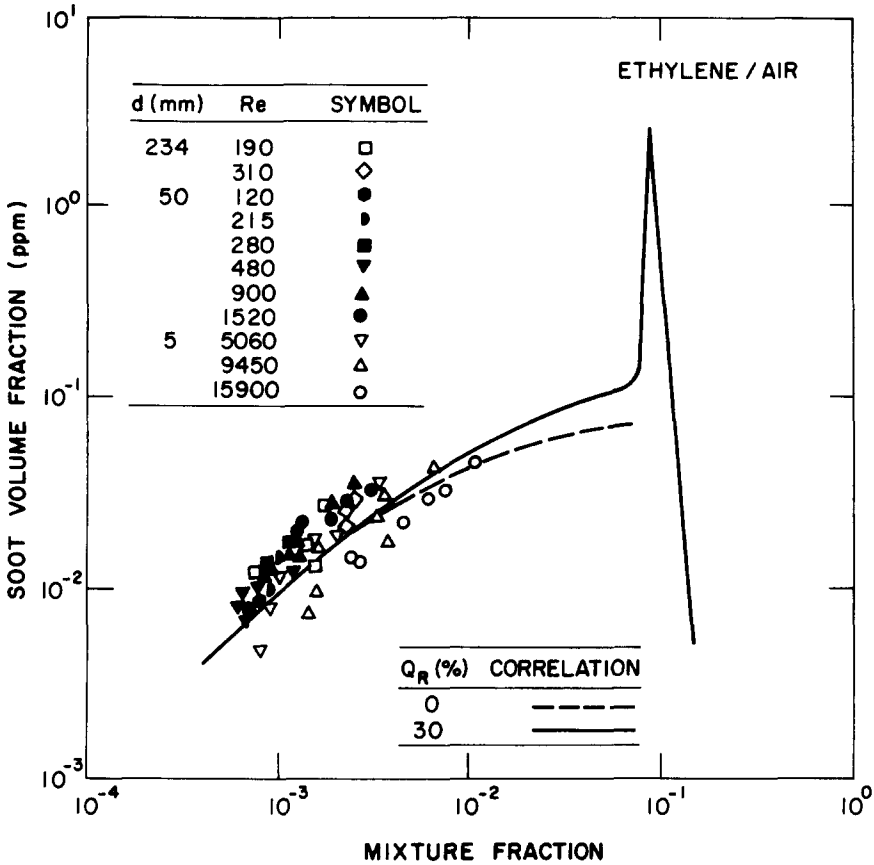

Fig. 7. Soot volume fraction state relationships for turbulent ethylene-air diffusion flames.

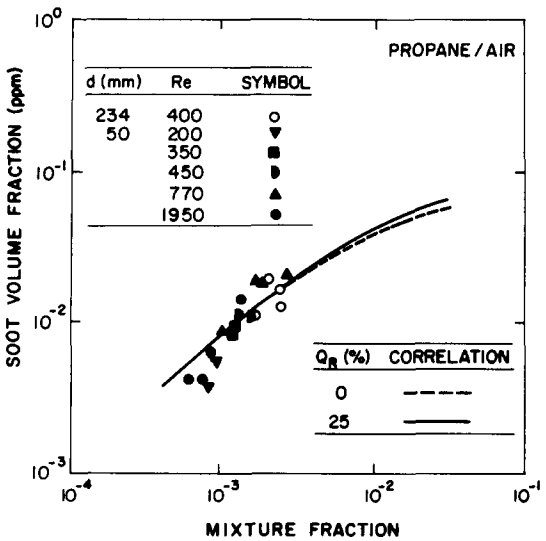

Fig. 8. Soot volume fraction state relationships for turbulent propane-air diffusion flames.

cations along the diffusion flame sheet and for various burner operating conditions. Because chemical phenomena and processes for fuel-rich conditions within the soot spike influence properties at quenching, this observation provides potential for similar universality of soot volume fractions as a function of mixture fractions within the soot spike itself. However, universality at quenching is only a necessary, but not sufficient, condition for universality within the soot spike, which must still be studied.

The propylene measurements (Fig. 6) are qualitatively similar to acetylene, but an effect of flame scale can be seen, e.g., soot concentrations are consistently higher for the 50- and 234-mm-diameter burners than for the 5-mm-diameter burner. Furthermore, soot concentrations generally become smaller as the Reynolds number increases for the 5-mm-diameter burner, which par-

allels reduced residence times with increasing Reynolds numbers for this burner (note that the effect of Reynolds number on residence time is generally just the opposite for the larger burners, see Fig. 4). Nevertheless, results for a particular flame residence time (Reynolds number and burner diameter) tend to have the same soot generation efficiency at all points in the overfire region suggesting that a particular flame residence time is representative of the flame as a whole, even though soot enters the overfire region from a variety of points along the flame sheet—each point presumably having a different residence time.

Results for ethylene (Fig. 7) continue the trend of increasing departure from a universal state relationship for soot volume fractions in the overfire region with reduced tendency to soot of the fuel. Results for the two large burners, at the longer flame residence times, correlate quite well, but results at shorter residence times for the 5 mm diameter burner are consistently lower and soot concentrations progressively decrease as the Reynolds number increases (which implies reduced residence times for this burner). Finally, similar to propylene, soot generation efficiencies tend to be relatively constant throughout the overfire region for a particular burner diameter and Reynolds number.

Propane had the lowest propensity to soot for the test conditions considered during the present investigation. Results for propane (Fig. 8) exhibit less tendency to scatter from a universal state relationship for soot volume fractions than ethylene; however, this is largely due to a reduced range of burner conditions for propane. Soot generation efficiencies for propane were relatively constant throughout the overfire region for a particular flame but progressively decreased as the flame residence time was decreased similar to the other fuels. In fact, measurements could not be obtained with the 5-mm-diameter burner for propane since the short residence times for this burner yielded very low soot concentrations that could not be accurately measured using present methods.

The results illustrated in Figs. 5–8 indicate that the laminar flamelet concept for soot volume fractions in the overfire region becomes progressively more satisfactory in the order propane, ethylene, propylene, and acetylene. This is the same order as the propensity of the fuels to soot, as represented by normal smoke point flame heights [35]. This suggests that residence times at the normal smoke point might be a useful measure of residence times needed for the laminar flamelet approximation for soot volume fractions to be appropriate. This prompted present measurements of smoke point properties using the methods described earlier.

TABLE 2

Normal Smoke Point Properties of the Fuels[a]

	Acetylene	Propylene	Ethylene	Propane
Schug et al. [35][b]				
Flame height (mm)	19	29	106	162
Present[c]				
Flame height (mm)	30	36	135	169
Residence time (ms)	14	16	41	48
Fuel flow rate (ml/s)	0.87	0.97	4.79	4.19

[a] Combustion in air with reactants at normal temperature and pressure.

[b] Flames stabilized on a 10-mm-diameter burner with air coflow in region where normal smokepoint flame height is nearly independent of the rate of coflow.

[c] Flame stabilized on a 14.3 mm diameter burner with 967 ml/s air coflow through a concentric port having an inside diameter of 102 mm.

Present measurement of flame heights and residence times at the normal smoke point, as well as the earlier measurements of smoke point flame heights by Schug et al. [35], are summarized in Table 2. Present smoke point flame heights vary in the same order but are somewhat longer than those of Ref. 35. This is attributed to different coflow velocities. In particular, the present open flames in relatively slow coflowing air have lower rates of flame stretch at their tips than the coflowing duct flames of Schug et al. [35]. This tends to reduce quenching of soot oxidation reactions near the flame tip, allowing somewhat longer flame lengths before soot begins to pass into the overfire region. For example, smoke point flame heights

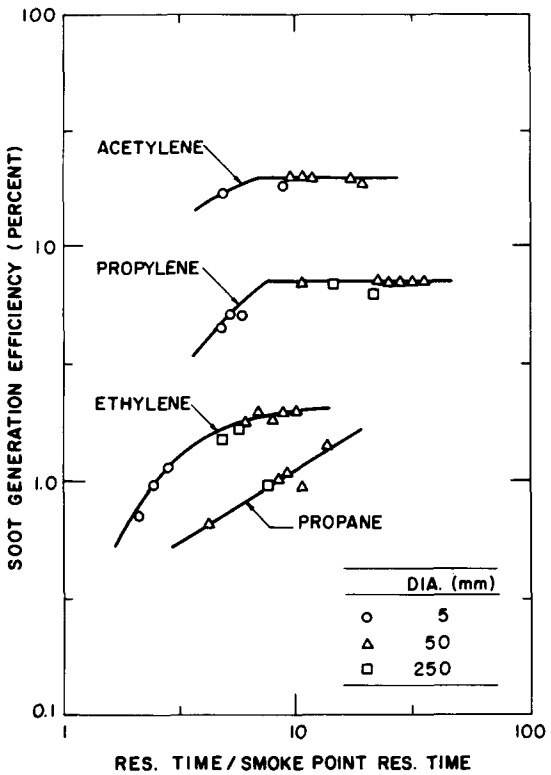

Fig. 9. Soot generation efficiencies as a function of residence times for turbulent acetylene, propylene, ethylene, and propane diffusion flames burning in air.

for acetylene and propylene could be observed with no coflow, yielding values of 38- and 54-mm, as opposed to the lower flame heights with coflow, e.g., 30 and 36 mm. Flame residence times at the normal smoke point vary in the same order as the flame heights but are much smaller than the residence times of the present turbulence test flames. Thus, even though the smoke point residence times vary somewhat for different experimental conditions, they still provide a reasonable measure of residence times needed for flames to begin emitting soot. This is examined in the following.

As noted earlier, soot generation efficiencies were relatively independent of position in the flame but varied with fuel type and operating conditions. Thus, an average soot generation efficiency could be found for each flame and associated with its residence time. Plots of the resulting soot generation efficiencies as a function of residence time, normalized by the smoke point residence time, are illustrated in Fig. 9.

The results illustrated in Fig. 9 indicate that soot generation efficiencies correlate reasonably well with flame residence times for a wide range of burner sizes and operating conditions for a particular fuel. Soot generation efficiencies increase at first with increasing residence time but then become nearly constant within an asymptotic (plateau) region for residence times longer than roughly ten times the smoke point residence time for acetylene, propylene, and ethylene. We were not able to reach a plateau condition for propane; however, results discussed below suggest the onset of such a regime at slightly longer residence times than present measurements. The soot volume fraction state relationship in the overfire region is universal in the long residence time plateau regime because soot generation efficiencies are independent of flame operating conditions and position in the overfire region—at least for the range of conditions considered during the present investigation.

Becker and Liang [20] considered soot yields from hydrocarbon-air flames using a sampling probe along the axis. Results for methane, ethane, propane, ethylene, and acetylene were correlated to give soot-yield factors (which are proportional to soot generation efficiencies) as functions of either Richardson ratios or first-Damkohler ratios (see Becker and Liang [20] for their definitions of these parameters). Their results also exhibited a tendency for soot yield factors to approach constant values at large first-Damkohler ratios (which is a measure of residence time) similar to the results illustrated in Fig. 9. A disturbing feature of measurements of Becker and Liang [20], however, is that soot-yield factors for acetylene tended to decrease once again for very large first-Damkohler ratios. This behavior, however, is probably due to the fact that Becker and Liang [20] computed the first-Damkohler ratio from burner operating conditions rather than directly measuring flame residence times. As buoyant jet flame conditions are approached, residence time scaling laws change and it is probable that results for the largest first-Damkohler ratios of Becker and Liang [20] actually involve shorter residence times than results in their plateau region. Present test conditions for acetylene overlap those of Becker and Liang [20] and the fact that there was no tendency for soot

TABLE 3

Soot Generation Efficiencies for Sooting Turbulent Diffusion Flames[a]

Source	Acetylene	Propylene	Ethylene	Propane
Present study[b,c]				
5-mm burner	0.17 (0.03)	0.048(0.008)	0.01(0.003)	—
50-mm burner	0.19 (0.04)	0.067(0.011)	0.018(0.003)	0.010(0.004)
234-mm burner	—	0.066(0.012)	0.016(0.003)	0.010(0.002)
Asymptotic Value	0.20	0.069	0.019	—
Sivathanu et al. [18][b,c]	0.11 (0.07)	—	0.010(0.006)	—
Gore and Faeth [3, 4]	0.21	—	0.012	—
Newman and Steciak [34]	—	0.063	0.017	0.021
Becker and Liang [20][d]	0.10	—	0.045	0.0045

[a] For turbulent diffusion flames in still air at normal temperature and pressure.

[b] Estimated from soot volume fraction measurements using a soot density of 1100 kg/m^3 from Newman and Steciak [34].

[c] Numbers in parentheses denote standard deviations.

[d] For characteristic residence times, defined by Becker and Liang [20], greater than 70 s for acetylene, 180 s for ethylene, and 180 s for propane.

generation efficiencies to decline again at long residence times tends to support this explanation.

Soot generation efficiencies measured during the present investigation are summarized in Table 3, along with earlier measurements of Sivathanu et al. [18], Gore and Faeth [3, 4], Newman and Steciak [34], and Becker and Liang [20]. Present measurements are summarized for each burner along with the more relevant asymptotic value obtained from Fig. 9. As noted earlier, no asymptotic value was found for propane for present test conditions. Standard deviations of the present measurements, and those of Ref. 18, are noted in parenthesis.

In view of potential effects of flame geometry, residence times, and experimental uncertainties, the agreement between the various determinations of soot generation efficiencies in Table 3 is reasonably good. In particular, the present asymptotic soot generation efficiency for acetylene is in good agreement with Gore and Faeth [3], although both these values are larger than Sivathanu et al. [18], which exhibit greater experimental uncertainties. Present asymptotic values of soot generation efficiencies for propylene and ethylene are also in good agreement with the values reported by Newman and Steciak [34]; residence times for the latter test flames are not known but these flames were large and were probably within the plateau region. Present soot generation efficiencies for propane are smaller than the measurements of Newman and Steciak [34], reflecting that the present flames did not reach a plateau condition that may have been achieved by Newman and Steciak [34] with their large flames. Additional study of propane and other alkanes would be desirable to gain a better understanding of their long residence time soot properties. The measurements of Becker and Liang [20] are generally lower than the rest, probably due to incomplete collection of soot, which is a common problem with probe sampling methods.

Taken together, both present and earlier studies support the view that soot mixes passively in the overfire region, with little change of optical properties, for a wide variety of flame conditions. Furthermore, the behavior of soot volume fractions in the overfire region is consistent with soot generation efficiencies being largely a function of flame residence time, and becoming constant for long flame residence times, for a particular fuel and ambient conditions. Finally, operation in the long residence time regime involves a universal state relationship for soot volume fractions, which provides a useful simplification for analysis of the continuum radiation properties of the overfire region.

CONCLUSIONS

The soot volume fraction state relationship concept was studied experimentally in the overfire region of turbulent acetylene, propylene, ethylene, and propane diffusion flames burning in still air. Measurements of related properties, like flame heights and characteristic flame residence times, were also undertaken for the same flames. The main conclusions of the study are as follows:

1. Soot generation efficiencies were uniform throughout the overfire region for a given fuel and operating condition, implying that a single state relationship for soot volume fractions applies to the entire overfire region; and that soot volume fractions and mixture fractions, when soot oxidation quenches, are independent of position within the flame.
2. Soot generation efficiencies were largely a function of characteristic flame residence time. Furthermore, soot generation efficiencies increased with increasing characteristic flame residence times but tended to approach asymptotic values for characteristic residence times roughly ten times longer than those at the normal smoke point. Within the asymptotic region (which includes most buoyant turbulent diffusion flames for heavily sooting materials like acetylene) the soot volume fraction state relationship is universal, offering substantial simplifications for analysis of continuum radiation in the overfire region. Additionally, these observations are consistent with the optical properties of soot being relatively independent of residence time and position in the overfire region.
3. Present measurements of soot generation efficiencies were in good agreement with Gore and Faeth [3, 4] and Newman and Steciak [34]. Earlier measurements of Becker and Liang [20] were lower, an effect that was attributed to problems of mechanical sampling of soot during these studies.
4. Present buoyant flames having $L/d < 20$ were in good agreement with the flame height correlation of Zukoski et al. [27]. These same flames yielded a reasonably good correlation for characteristic residence times, which is an important parameter for assessing whether a flame is in the asymptotic region where soot generation efficiencies are constant.

Conclusions with respect to soot properties are based on the Rayleigh approximation of small particles and the use of a single set of refractive indices from Dalzell and Sarofim [5]: additional assessment of the small particle limit and information about the refractive index properties of soot in diffusion flames would be desirable to help resolve potential effects of the fuel, temperatures and residence times [1, 5–9]. Nevertheless, further evaluation of the soot volume fraction state relationship concept appears to be warranted. The main priorities are to study the concept for a wider range of fuels and ambient conditions, and in the underfire region.

This research was supported by the Center for Fire Research of the National Institute of Standards and Technology (formerly the National Bureau of Standards), Grant No. 60NANB5D0526 and 60NANB8D0833, with D. D. Evans and H. Baum serving as Scientific Officers.

REFERENCES

1. Tien, C. L., and Lee, S. C., *Prog. Ener. Combust. Sci.* 8:41–59 (1982).
2. Flower, W. L., and Bowman, C. T., *Twenty-First Symposium (International) on Combustion*, The Combustion Institute, Pittsburgh, 1986, p. 1115.
3. Gore, J. P., and Faeth, G. M., *J. Heat Trans.* 110:173–181 (1988).
4. Gore, J. P., and Faeth, G. M., *Twenty-First Symposium (International) on Combustion*, The Combustion Institute, Pittsburgh, 1986, p. 1521.
5. Dalzell, W. H., and Sarofim, A. F., *J. Heat Trans.* 91:100–104 (1969).
6. Batten, C. E., *Appl. Opt.* 24:1193–1199 (1985).
7. Charalampopoulos, T. T., and Felske, J. D., *Combust. Flame* 68:283–294 (1987).
8. Charalampopoulos, T. T., and Chang, H., *Combust. Sci. Technol.* 59:401–421 (1988).
9. Habib, Z. G., and Vervisch, P., *Combust. Sci. Technol.* 59:261–274 (1988).
10. Bilger, R. W., *Combust. Flame* 30:277–284 (1977).
11. Liew, S. K., Bray, K. N. C., and Moss, J. B., *Combust. Sci. Technol.* 27:69–73 (1981).

12. Liew, S. K., Bray, K. N. C., and Moss, J. B., *Combust. Flame* 56:199–213 (1984).
13. Faeth, G. M., and Samuelsen, G. S., *Prog. Ener. Combust. Sci.* 12:305–372 (1986).
14. Gore, J. P., Jeng, S.-M., and Faeth, G. M., *J. Heat Trans.* 109:165–171 (1987).
15. Gore, J. P., Jeng, S.-M., and Faeth, G. M., *AIAA J.* 25:339–345 (1987).
16. Jeng, S.-M., and Faeth, G. M., *J. Heat Trans.* 106:721–727 (1984).
17. Jeng, S.-M., and Faeth, G. M., *J. Heat Trans.* 106:891–893 (1984).
18. Sivathanu, Y. R., Gore, J. P., and Faeth, G. M., *Combust. Flame* 73:315–329 (1988).
19. Jeng, S.-M., Ph.D. thesis, The Pennsylvania State University, University Park, PA, 1984.
20. Becker, H. A., and Liang, D., *Combust. Flame* 44:305–318 (1982); 52:247–256 (1983).
21. Gore, J. P., Ph.D. thesis, The Pennsylvania State University, University Park, PA, 1986.
22. Santoro, R. J., Dobbins, R. A., and Semerjian, H. G., *Prog. Astronaut. Aeronaut.* 92:343–382 (1984).
23. Megaridis, C. M., and Dobbins, R. A., *Twenty-Second Symposium (International) on Combustion*, The Combustion Institute, Pittsburgh, 1988, p. 353.
24. Santoro, R. J., Semerjian, H. G., and Dobbins, R. A., *Combust. Flame* 51:203–218 (1983).
25. Flower, W. L., *Twenty-Second Symposium (International) on Combustion*, The Combustion Institute, Pittsburgh, 1988, p. 425.
26. deRis, J., *Seventeenth Symposium (International) on Combustion*, The Combustion Institute, Pittsburgh, 1978, p. 1003.
27. Zukoski, E. E., Cetegen, B. M., and Kubota, T., *Twentieth Symposium (International) on Combustion*, The Combustion Institute, Pittsburgh, 1984, p. 361.
28. McCaffrey, B. J., NBSIR79-1910, National Institute of Standards and Technology, Washington, 1979.
29. Steward, F. R., *Combust. Sci. Technol.* 2:203–212 (1970).
30. Terai, T., and Nitta, K., *Proc. Syms. Arch. Inst. Jpn.* (1975).
31. Thomas, P. H., *Ninth Symposium (International) on Combustion*, The Combustion Institute, Pittsburgh, 1962, p. 844.
32. You, H.-Z., and Faeth, G. M., *Fire Materials* 3:140–147 (1979).
33. Kent, J. H., *Combust. Flame* 67:223–233 (1987).
34. Newman, J. S., and Steciak, J., *Combust. Flame* 67:55–64 (1987).
35. Schug, K. P., Manheimer-Timnat, Y., Yaccarino, P., and Glassman, I., *Combust. Sci. Technol.* 22:235–250 (1980).

Received 6 February 1989; revised 13 September 1989